A Novel Fast Fixed-Time Backstepping Control of DC Microgrids Feeding Constant Power Loads

Sarrafan, Neda; Zarei, Jafar; Horiyat, Navid; Razavi-Far, Roozbeh; Saif, Mehrdad; Mijatovic, Nenad; Dragičević, Tomislav

Published in:
IEEE Transactions on Industrial Electronics

Link to article, DOI:
10.1109/TIE.2022.3192669

Publication date:
2023

Document Version
Peer reviewed version

A Novel Fast Fixed-Time Backstepping Control of DC Microgrids Feeding Constant Power Loads

Neda Sarrafan, Jafar Zarei, *Member, IEEE*, Navid Horiyat, Roozbeh Razavi-Far, *Senior Member, IEEE*, Mehrdad Saif, *Senior Member, IEEE*, Nenad Mijatovic, *Senior Member, IEEE* and Tomislav Dragičević, *Senior Member, IEEE*

***Abstract*—Nonlinear behavior of constant power loads (CPLs) and their negative incremental impedance, which impose adverse effects on system damping and stability margins, necessitate developing proper strategies for efficient implementation framework of DC microgrid. In this paper, a fixed-time sliding mode disturbance observer (SMDO) is first addressed to provide an estimation of the instantaneous power flow moving along the uncertain CPLs with time-varying nature within a fixed time. It not only expedites the estimation rate but also improves the robustness against physical parameter variation. The fast fixed-time backstepping technique is then developed based on the estimated load power to control the duty cycle of the boost converter such that the entire power grid becomes stable and the desired voltage of the DC bus is tracked within a fixed time irrespective of the initial conditions. A rigorous Lyapunov-based approach is represented to guarantee the fixed-time stability of the proposed scheme. Finally, to validate the merits and implementation feasibility of the proposed methodology, the experimental realization is represented under various operating case studies.**

***Index Terms*—DC microgrid, Constant power load, Fixed-time disturbance observer, Fast Fixed-time Backstepping controller, Experimental test.**

NOMENCLATURE

v_C	Capacitor voltage
i_L	Inductor current
L	Inductance of the DC/DC boost converter
C	Capacitance of the DC/DC boost converter
R_s	Resistance of the resistive load
R_0	Nominal resistance of the resistive load
V_{in}	Input voltage
P_{CPL}	Power of the CPL
v_{CPL}	Voltage of the CPL
i_{CPL}	Current of the CPL
η	Duty cycle of the switch signal
y_1	Total stored electrical energy
y_2	New state variable
δ_1	Mismatched disturbance
δ_2	Matched disturbance
u	Intermediate control law
$v_{C,d}$	Desired capacitor voltage
$i_{L,d}$	Desired inductor current
$k_1, k_2, \ldots, k_6$	Disturbance observer gains
m_1, m_2, m_3	Disturbance observer parameters
n_1, n_2, n_3	Disturbance observer parameters
$\hat{\delta}_1$	Mismatched disturbance estimation
$\hat{\delta}_2$	Matched disturbance estimation
$\alpha_1, \alpha_2, \beta_1, \beta_2$	Controller gains
m, n, p, q	Controller parameters

Manuscript received Mar 24, 2022; revised July 14, 2022; accepted MM dd, 2022. (*Corresponding Author: J. Zarei*)

N. Sarrafan is with the Department of Electrical and Electronics Engineering, Shiraz University of Technology, Shiraz, Iran (e-mail: n.sarrafan@sutech.ac.ir).

J. Zarei is with the Department of Electrical and Electronics Engineering, Shiraz University of Technology, Shiraz, Iran, and also is with the Department of Electrical and Computer Engineering, Windsor University, On N9B 3P4, Canada (e-mails: zarei@sutech.ac.ir, jzarei@uwindsor.ca).

N. Horiyat is with the Department of Electrical Engineering, Jasb Branch, Islamic Azad University, Jasb, Iran (e-mail: n.horiyat@iaujasb.ac.ir).

R. Razavi-Far and M. Saif are with the Department of Electrical and Computer Engineering, Windsor University, On N9B 3P4, Canada. (e-mail: roozbeh@uuwindsor.ca and msaif@uniwindsor.ca).

N. Mijatovic and T. Dragičević are with Elektro, Danmark Technical University, 5205 Lyngby, Denmark, (e-mail: nm@elektro.dtu.dk and tomdr@elektro.dtu.dk).

I. INTRODUCTION

MAJOR breakthroughs have been made in global energy development during the past decade. Depletion of fossil fuel reserves and environmental issues encourages conventional power systems to take advantages of the distributed generations containing renewable energy sources, energy storage systems, and various types of loads. The effective integration of distributed generators can be facilitated by microgrids (MGs). DC characteristics of most renewable energy sources and a surge in DC demand have put increased attention on DC microgrids with wide applications such as in shipboard power systems [1], electric aircraft [2], and hybrid electric vehicles [3]. Moreover, high efficiency, reliability, scalability, and fault reconfigurability make DC MGs a preferable architectural option in comparison with the AC ones [4]. The key control objective of the MG system is to ensure the desired voltage regulation in all operating conditions. A hierarchical three-layer control scheme has been introduced to control microgrids in three major levels, primary, secondary, and tertiary control [5]. Subsequent to the islanding process, the primary control ensures the voltage and frequency stability of the microgrid at the lowest level. Moreover, preserving the balance of power-sharing is essential for the distributed energy resources in the presence of various types of loads. This primary control level deals with the inner voltage and current control loops of the DERs. Secondary control has been widely used to compensate for the frequency and voltage deviations due to the operation of the primary controls. Finally, the tertiary level is responsible for managing the power flow between the microgrid and the main grid and provides an optimal operation.

In the DC microgrid setting, the tightly-regulated power electronic interfaces act as constant power loads, which are nonlinear with negative impedance V-I characteristics resulting in instability of the power grid [6]. Such instabilities induced by CPLs impose dire effects including a reduction in system damping and high inrush current [7]. To increase the damping factor, three passive damping circuits including RC parallel, RL series, and RL parallel have been represented in [8]. However, passive damping approaches suffer from heavy losses and costs. Another solution to mitigate negative impedance characteristics exhibited by CPLs would be active damping methods in which large virtual resistance is connected in parallel or series with the input impedance of the load converter [9]. However, by adopting the linear small-signal model, the DC MG can only be stabilized near nominal operating points. Besides, the power injection may degrade the load performance.

In a large-signal sense, numerous nonlinear strategies such as feedback-linearization technique [10], [11], sliding-mode control [12–14], backstepping control [15], [16], model predictive control [17], fuzzy method [18], combination of fuzzy with model predictive control [19], deep deterministic reinforcement learning [20], passivity-based control [21] have been conducted to minimize destabilization effects of CPLs on the DC microgrids. It can be observed that the represented schemes [10–21] stabilize the entire power system with an asymptotical convergence rate in infinite time, which may not be adequate for abrupt changes in various system operating states and step-wise load variations. One way of overcoming this challenge is to establish a finite-time control method, which not only accelerates the convergence rate but also provides strong robustness in the face of uncertainties, and improved disturbance attenuation. In [22], a composite finite-time protocol containing a finite-time disturbance observer and a finite-time backstepping controller is developed for stabilizing a DC/DC boost converter loaded by CPLs. In [23] a finite-time control protocol is presented for accurate power sharing and voltage regulation of super capacitor system feeding CPLs by employing a non-recursive synthesis strategy based on rigorous large-signal stability analysis. In [24], integer and fractional order terminal sliding mode control laws are established for DC/DC boost converter to overcome the instability challenge caused by constant power loads. However, in the introduced techniques in [22–24], the upper-bound estimate for settling time relies on the initial conditions. From a practical point of view, DC bus voltage deviation for larger initial states can result in power loss. Thus, it is desirable to expedite the convergence rate regardless of initial states that can be satisfied by proposing a fixed-time control technique. In [25], the fixed-time terminal sliding mode controller is suggested to stabilize the entire marine power grid as well as tracking the reference voltage of the DC bus in the fixed time. However, the convergence time of this control technique can not be considered an optimal one. Thus, it is essential to design the controller which ensures fast convergence rate both far away from and at a close range of the control objective.

Moreover, putting forward a promising solution to compensate for the adverse effect of uncertainties in the power of CPLs is an absolute necessity in the high-performance control of modern power grids. To measure the capacitor current of the output filter, a current sensor is required to be installed in series with the capacitor, leading to higher equivalent series resistance. Besides, the installation of additional sensors gives rise to system cost and complexity. In [26], [27], the uncertainty in the power load is only assumed to be bounded by a certain positive constant. An alternative method to deal with these limitations can be developing the estimation techniques to provide instantaneous power estimation of CPLs. Deterministic observers [15], [25], [28] and stochastic filters [17] are recognized as two general types of power load estimators. In [15], [28], nonlinear disturbance observers have been designed to estimate the time-varying load power changes asymptotically in infinite time. To speed up the estimating process, a finite-time disturbance observer is suggested in [25], which provides load power estimation in the finite time. However, the upper bound of convergence time depends on the initial conditions.

This paper presents a new fast fixed-time disturbance observer-based backstepping controller for the voltage regulation of DC/DC boost converter loaded by uncertain CPLs in a fixed time irrespective of initial conditions. The significant contributions of this paper can be outlined as:

1) Unlike [10–21] in which voltage regulation of DC MGs with uncertain CPLs is asymptotically accomplished, the proposed strategy guarantees the fixed-time stability of DC MGs to mitigate the instability impact of the CPLs as fast as possible;
2) According to the best knowledge of authors [25–28], the fixed-time sliding-mode disturbance observer (SMDO) has not been yet proposed for DC MGs to estimate the changes of CPL in a fixed time. It not only expedites the estimation rate by eliminating the dependence on the initial conditions but also enhances the estimation robustness against physical parameters variation such as system capacitance, inductance, and resistance by adopting sigmoid functions in the observer framework. It can also decrease the implementation cost, size, and weight of the system compared to sensors installation;
3) The fast fixed-time backstepping controller (FFTBC) is constructed for the first time to not only stabilize the system within a fixed time but also ensure a fast optimal convergence rate both far away from and at a close range of the reference voltage;
4) The proposed protocol is implemented by establishing an experimental setup in which the complexity of the plant under control is included. A comparative study is carried out to highlight the superiorities of the constructed scheme.

The remainder of this work is arranged as follows: Section II provides the dynamic model of DC microgrids. The control objectives are first explained in Section III. Then, after introducing a coordinate transformation, the observer-based control strategy is established. Section IV demonstrates the real-time outcomes and examines the efficiency of the proposed approach. Finally, Section V concludes the paper.

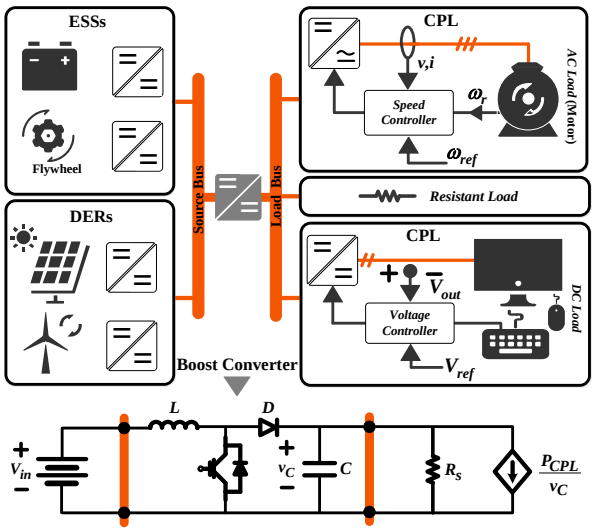

Fig. 1. Typical topology of DC microgrids and its equivalent circuit diagram

II. Configuration of DC Microgrid

Fig. 1 depicts the schematic diagram of a DC microgrid and its equivalent circuit. The environmental and economic issues result in a global trend toward more utilization of renewable energy sources such as photovoltaics, which is DC in nature, and wind turbine, which is integrated into the AC grid through a DC link. However, the weather conditions and geographic locations may cause intermittency in solar and wind energy. To address this unreliability, static storage integration is carried out by employing purely DC elements such as batteries and mechanical energy storage systems such as flywheels. On the load side, if the control bandwidth of the tightly-controlled power electronic converter feeding load is high enough, it can act as a constant power load, which can be DC or AC supplied.

The DC/DC boost converter feeding CPLs and resistive loads are illustrated in Fig. 1. The dynamic equation of the system is accomplished by employing Kirchhoff's laws:

$$\begin{cases} \frac{dv_C}{dt} = \frac{1}{C}\left[(1-\eta)\, i_L - \frac{v_C}{R_s} - \frac{P_{CPL}}{v_C}\right] \\ \frac{di_L}{dt} = \frac{1}{L}\left[V_{in} - (1-\eta)\, v_C\right] \end{cases} \tag{1}$$

where L and C are the boost converter parameters, i_L is the inductor current, v_C is the voltage of the capacitor, $P_{CPL} = v_{CPL} i_{CPL}$ is the power of the CPL, V_{in} is the input voltage and η denotes the duty ratio of the control switch signal, which implies the control input of the system.

III. Fast Fixed-Time Disturbance Observer-Based Backstepping Controller

In this part, the main control objectives are explained at first and the system model given in (1) is converted into Brunovsky's canonical form. Then, the fixed-time SMDO is formulated to track the possible variation of the power load produced by the non-ideal CPLs. Finally, the fast fixed-time backstepping is proposed to make the system states converge to the desired equilibrium points within a fixed time.

A. Control Objectives

The current drawn by CPLs increases/decreases when its terminal voltage decreases/increases leading to a negative incremental impedance [29]. Thus, a reduction in the effective damping of the system is made resulting in system instability. The most critical situation of system stability may occur under pure CPL. That is why the resistive loads are employed to enhance the system damping [29]. Besides, the nonlinear behavior of CPLs necessitates investigating proper strategies to ensure system stability. The major control target is to design the control signal η such that the fixed-time convergence property regardless of the initial states are provided for the output voltage v_C to follow its desired value $v_{C,d}$. The duty cycle for pulse-width modulator (PWM) control of the boost converter can be obtained by the output signal of the controller.

Definition 1: For systems (1), a fixed-time tracking can be obtained to restore the voltage deviation caused by constant power loads if there exists a proper control signal η such that $\lim_{x \to T} v_C = v_{C,d}$ and $v_C = v_{C,d}$, $\forall t \geq T$ where T is independent of the initial value of the voltage.

B. Diffeomorphism Coordinate Transformation

To design the proposed fast fixed-time backstepping controller, Brunovsky's canonical form of the dynamic model in (1) is required [30]. A diffeomorphism transformation generates the standard form of the integrator system with the new coordinate of the total stored energy and rate of change of stored energy, respectively.

In the dynamic system (1), capacitor C and inductor L are the energy storage units. The total stored energy is expressed:

$$y_1 = \frac{1}{2}\left(L i_L^2 + C v_C^2\right) \tag{2}$$

Its time derivative can be taken by considering (1) as:

$$\dot{y}_1 = L i_L \frac{di_L}{dt} + C v_C \frac{dv_C}{dt} = V_{in} i_L - \frac{v_C^2}{R_s} - P_{CPL} \tag{3}$$

A new variable y_2 and the uncertain term δ_1 are defined:

$$y_2 = V_{in} i_L - \frac{v_C^2}{R_0} \tag{4}$$

$$\delta_1 = -P_{CPL} + \frac{v_C^2}{R_0} - \frac{v_C^2}{R_s} \tag{5}$$

In practice, the nominal resistance of the resistive load R_0 should be also considered since uncertain environmental factors like temperature may affect the load resistance R_s. Taking the time derivative y_2 leads to the following result:

$$\begin{aligned} \dot{y}_2 = {} & \frac{V_{in}^2}{L} + \frac{2v_C^2}{R_0^2 C} - \left(\frac{V_{in} v_C}{L} + \frac{2 i_L v_C}{R_0 C}\right)(1-\eta) \\ & + \frac{2}{R_0 C}\left(P_{CPL} - \frac{v_C^2}{R_0} + \frac{v_C^2}{R_s}\right) \end{aligned} \tag{6}$$

Based on (6), by isolating the unknown values including the total amount of load power, u and δ_2 are denoted as:

$$u = \frac{V_{in}^2}{L} + \frac{2v_C^2}{R_0^2 C} - \left(\frac{V_{in} v_C}{L} + \frac{2 i_L v_C}{R_0 C}\right)(1-\eta) \tag{7}$$

$$\delta_2 = \frac{2}{R_0 C}\left(P_{CPL} - \frac{v_C^2}{R_0} + \frac{v_C^2}{R_s}\right) \tag{8}$$

The following standard form of integrator systems is finally achieved by employing the aforementioned transformation to the dynamic system model:

$$\begin{cases} \dot{y}_1 = y_2 + \delta_1 \\ \dot{y}_2 = u + \delta_2 \end{cases} \tag{9}$$

The main control objective is to design the control law η so that DC bus voltage v_C can track its reverence value $v_{C,d}$ within a fixed time. After employing the coordinate transformation, the intermediate control law u should be designed such that state y_1 tracks its reference value $y_{1,d}$ which is given by:

$$y_{1,d} = \frac{1}{2}(Li_{L,d}^2 + Cv_{C,d}^2) = \frac{1}{2}L(\frac{P_{Load}}{V_{in}})^2 + \frac{1}{2}Cv_{C,d}^2 \tag{10}$$

The load power including resistive load and CPL is derived:

$$P_{Load} = P_{CPL} + \frac{v_{C,d}^2}{R_s} \tag{11}$$

The intermediate control input u should be proposed such that the fixed-time stability of (9) is guaranteed. Afterwards, the main control input η in system (1) is obtained from (7):

$$\eta = 1 - (\frac{V_{in}^2}{L} + \frac{2v_C^2}{R_s^2 C} - u)/(\frac{V_{in}v_C}{L} + \frac{2v_C i_L}{R_s C}) \tag{12}$$

C. Fixed-time SMDO for Power Estimation

Based on (5) and (8), the disturbance terms δ_1 and δ_2 are mainly due to the output power variation and are required to be estimated within a fixed time. Accordingly, the fixed-time SMDO structure is constructed to estimate the mismatched disturbance δ_1 in (9) as follows [31–33]:

$$\begin{cases} \dot{\sigma}_1 = \sigma_2 - k_1 sig^{m_1}(\sigma_1 - y_1) - k_2 sig^{n_1}(\sigma_1 - y_1) + y_2 \\ \dot{\sigma}_2 = \sigma_3 - k_3 sig^{m_2}(\sigma_1 - y_1) - k_4 sig^{n_2}(\sigma_1 - y_1) \\ \dot{\sigma}_3 = -k_5 sig^{m_3}(\sigma_1 - y_1) - k_6 sig^{n_3}(\sigma_1 - y_1) \end{cases} \tag{13}$$

For any $i = 1, 2, 3$, the parameters $m_i \in (0, 1)$, $n_i > 1$ satisfy $m_i = i\bar{m} - (i-1)$, $n_i = i\bar{n} - (i-1)$, where $\bar{m} \in (1 - l_1)$, $\bar{n} \in (1 + l_2)$ for sufficiently small constants $l_1 > 0$, $l_2 > 0$. The observer gains k_i, $i = 1, 2, \ldots, 6$ should be designed such that the following matrices are Hurwitz:

$$A_1 = \begin{pmatrix} -k_1 & 1 & 0 \\ -k_3 & 0 & 1 \\ -k_5 & 0 & 0 \end{pmatrix}, \quad A_2 = \begin{pmatrix} -k_2 & 1 & 0 \\ -k_4 & 0 & 1 \\ -k_6 & 0 & 0 \end{pmatrix} \tag{14}$$

Definition 2: For any non-negative real number λ and $x \in \Re$, the function $x \mapsto sig^{\lambda}(x)$ is defined as $sig^{\lambda}(x) = sign(x)|x|^{\lambda}$, where $sign(x)$ is the standard sign function.

The mismatched disturbance δ_1 is assumed to be differentiable and there exists a small enough constant ς such that $\left|\dot{\delta}_1\right| \leq \varsigma$ holds. $\sigma_1 = \hat{y_1}$, $\sigma_2 = \hat{\delta}_1$ and $\sigma_3 = \dot{\hat{\delta}}_1$ introduce the estimation of y_1, δ_1 and $\dot{\delta}_1$, respectively. In [31], it is proved that the error dynamics of the observer will converge in a fixed time, which implies there exists a time constant $T_o \geq t_0$, independent of the initial observer errors, such that $\hat{y}_1 = y_1$, $\hat{\delta}_1 = \delta_1$ and $\dot{\hat{\delta}}_1 = \dot{\delta}_1$ for any $t \geq T_o$. Besides, the matched disturbance δ_2 in (9) can be estimated using the proposed fixed-time SMDO. According to (8), $\hat{\delta}_2$ is obtained:

$$\hat{\delta}_2 = -\frac{2}{R_0 C}\hat{\delta}_1 \tag{15}$$

Taking into consideration (5), (11), and (13), the estimation of total amount of load power can be calculated as:

$$\hat{P}_{Load} = -\hat{\delta}_1 + \frac{v_{C,d}^2}{R_0} \tag{16}$$

Then, the reference value of state y_1 in (10) is reformulated:

$$y_{1,d} = \frac{1}{2}\frac{L}{V_{in}^2}(\frac{v_{C,d}^2}{R_0} - \hat{\delta}_1)^2 + \frac{1}{2}Cv_{C,d}^2 \tag{17}$$

The observer convergence rate has been identified as a major factor in the effectiveness of the whole control system. In most of the suggested disturbance observer structures, only the asymptotic or finite-time convergence of the estimation errors can be guaranteed. To improve the convergence rate of the disturbance observer to be independent of the initial observer errors, the fixed-time SMDO (13) is designed. Then, the estimated load power is transferred to the fast fixed-time backstepping controller to meet the control objectives.

Remark 1: The main aim of this work is to regulate the DC voltage of the boost-based microgrid feeding unknown time-varying CPL. Therefore, it is not required to consider the dynamic of the CPL in the plant model directly. It is worth noting that, in the current study, by applying an appropriate transformation the variations of the CPLs are assumed to be a disturbance. These variations are estimated by a novel fixed-time sliding mode disturbance observer within a fixed time and it is proved that the system is stable under variations of CPLs. This strategy will help us prevent possible challenges in practice especially when there are multiple CPLs in the grid.

D. Fast Fixed-time Backstepping Control Strategy

In this section, the fast fixed-time backstepping control law is presented considering the system model in the strict-feedback form expressed in (9) and the total load power estimated by the fixed-time SMDO in (13). To meet the control objectives described in Section III. A, the control law should be constructed such that the state variable y_1 in (2) converges to its desired value $y_{1,d}$ in (17) within a fixed time. It is simply equivalent to tracking the reference values of system states $v_{C,d}$ and $i_{L,d}$ by their actual ones v_C and i_L, respectively, in fixed time without dependence on initial states.

The backstepping control approach in two steps is presented based on Lemma 1 in the Appendix considering the total load power estimated by the fixed-time SMDO to provide fast fixed-time stability of tracking errors.

Step 1: Designing the virtual control law y_2^*

The tracking error and its time derivative are first introduced using (9) as follows:

$$z = y_1 - y_{1,d} \tag{18}$$

$$\dot{z} = y_2 + \delta_1 - \dot{y}_{1,d} \tag{19}$$

where y_2 is virtual control input. Let the Lyapunov function candidate as $V_1 = \frac{1}{2}z^2$ whose time derivative becomes:

$$\dot{V}_1 = z\dot{z} = z(y_2 + \delta_1 - \dot{y}_{1,d}) \tag{20}$$

The main objective is to design the virtual control law y_2^* which makes z converge to zero within a fixed time by using

the fixed-time SMDO in (13). According to Lemma 1, the appropriate virtual control expression can be selected as:

$$\begin{aligned} y_2^* &= -\alpha_1 z^{\frac{1}{2}+\frac{m}{2n}+\left(\frac{m}{2n}-\frac{1}{2}\right)sign(|z|-1)} - \beta_1 z^{\frac{p}{q}} - \hat{\delta}_1 + \dot{y}_{1,d} \\ &\triangleq -\Lambda_1 - \hat{\delta}_1 + \dot{y}_{1,d} \end{aligned} \tag{21}$$

where α_1 and β_1 are the positive real numbers and m, n, p, q are positive odd integers that satisfy $m > n$, $p < q$. By substituting (21) into (20), $\dot{V}_1$ can be rewritten as $\dot{V}_1 = z(-\Lambda_1 - \hat{\delta}_1 + \delta_1) = -z\Lambda_1$. As mentioned in part C of section III, the observer estimation error $\delta_1 - \hat{\delta}_1$ is fixed-time stable and becomes zero for any $t \geq T_o$.

Step 2: Designing the intermediate control law u

To backstep, a variable change is made by $\varepsilon = y_2 - y_2^*$, which gives $y_2 = \varepsilon - \Lambda_1 - \hat{\delta}_1 + \dot{y}_{1,d}$. Considering (19), the transformed representation can be achieved as follows:

$$\begin{cases} \dot{z} = \varepsilon - \Lambda_1 \\ \dot{\varepsilon} = u + \delta_2 + \frac{\partial \Lambda_1}{\partial z}(\varepsilon - \Lambda_1) + \dot{\hat{\delta}}_1 - \ddot{y}_{1,d} \end{cases} \tag{22}$$

Set the Lyapunov function as $V = V_1 + V_2 = \frac{1}{2}z^2 + \frac{1}{2}\varepsilon^2$. Taking account of (22), $\dot{V}$ can be expressed as follows:

$$\begin{aligned} \dot{V} &= z\dot{z} + \varepsilon\dot{\varepsilon} \\ &= z(\varepsilon - \Lambda_1) + \varepsilon(u + \delta_2 + \frac{\partial \Lambda_1}{\partial z}(\varepsilon - \Lambda_1) + \dot{\hat{\delta}}_1 - \ddot{y}_{1,d}) \end{aligned} \tag{23}$$

To achieve fixed-time stability with a fast convergence rate, the intermediate control law u can be designed as follows:

$$u = -z - \hat{\delta}_2 - \frac{\partial \Lambda_1}{\partial z}(\varepsilon - \Lambda_1) - \dot{\hat{\delta}}_1 - \Lambda_2 + \ddot{y}_{1,d} \tag{24}$$

in which $-\Lambda_2 \triangleq -\alpha_2 \varepsilon^{\frac{1}{2}+\frac{m}{2n}+\left(\frac{m}{2n}-\frac{1}{2}\right)sign(|\varepsilon|-1)} - \beta_2 \varepsilon^{\frac{p}{q}}$ is defined, where α_2 and β_2 are the positive real numbers. Thus, under the assumption $\alpha_1 = \alpha_2 = \alpha$ and $\beta_1 = \beta_2 = \beta$, (24) is substituted into (23), which leads to the following result:

$$\begin{aligned} \dot{V} &= -z\Lambda_1 - \varepsilon\Lambda_2 = -\alpha(z^{\frac{1}{2}+\frac{m}{2n}+\left(\frac{m}{2n}-\frac{1}{2}\right)sign(|z|-1)+1} \\ &+\varepsilon^{\frac{1}{2}+\frac{m}{2n}+\left(\frac{m}{2n}-\frac{1}{2}\right)sign(|\varepsilon|-1)+1}) - \beta(z^{\frac{p}{q}+1} + \varepsilon^{\frac{p}{q}+1}) \end{aligned} \tag{25}$$

Referring to part C of section III, fixed-time stability of the observer estimation error $\delta_2 - \hat{\delta}_2$ can be guaranteed for any $t \geq T_o$. Four different cases should be analyzed to demonstrate the fast fixed-time stability using Lemma 2 in Appendix.

(i) when $|z| \geq 1$ and $|\varepsilon| \geq 1$:

$$\begin{aligned} \dot{V} &= -\alpha(z^{\frac{m}{n}+1} + \varepsilon^{\frac{m}{n}+1}) - \beta(z^{\frac{p}{q}+1} + \varepsilon^{\frac{p}{q}+1}) \\ &= -\alpha((z^2)^{\frac{\frac{m}{n}+1}{2}} + (\varepsilon^2)^{\frac{\frac{m}{n}+1}{2}}) - \beta((z^2)^{\frac{\frac{p}{q}+1}{2}} + (\varepsilon^2)^{\frac{\frac{p}{q}+1}{2}}) \\ &\leq -\alpha\, 2^{\frac{\frac{m}{n}+1}{2}} 2^{\frac{1-\frac{m}{n}}{2}} V^{\frac{\frac{m}{n}+1}{2}} - \beta\, 2^{\frac{\frac{p}{q}+1}{2}} V^{\frac{\frac{p}{q}+1}{2}} \\ &= -\alpha_0 V^{\frac{\frac{m}{n}+1}{2}} - \beta_0 V^{\frac{\frac{p}{q}+1}{2}} \end{aligned} \tag{26}$$

(ii) when $|z| < 1$ and $|\varepsilon| < 1$,

$$\dot{V} = -\alpha\left(z^2 + \varepsilon^2\right) - \beta(z^{\frac{p}{q}+1} + \varepsilon^{\frac{p}{q}+1}) \leq -2\alpha V - \beta_0 V^{\frac{\frac{p}{q}+1}{2}} \tag{27}$$

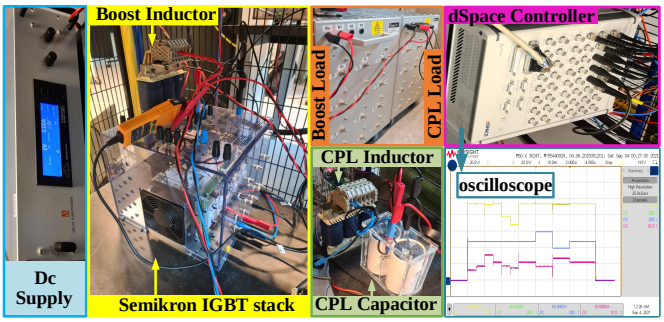

Fig. 2. Task diagram of experimental setup.

(iii) when $|z| \geq 1$ and $|\varepsilon| < 1$,

$$\begin{aligned} \dot{V} &= -\alpha(z^{\frac{m}{n}+1} + \varepsilon^2) - \beta(z^{\frac{p}{q}+1} + \varepsilon^{\frac{p}{q}+1}) \\ &\leq -\alpha((z^2)^{\frac{\frac{m}{n}+1}{2}} + (\varepsilon^2)^{\frac{\frac{m}{n}+1}{2}}) - \beta((z^2)^{\frac{\frac{p}{q}+1}{2}} + (\varepsilon^2)^{\frac{\frac{p}{q}+1}{2}}) \\ &\leq -\alpha_0 V^{\frac{\frac{m}{n}+1}{2}} - \beta_0 V^{\frac{\frac{p}{q}+1}{2}} \end{aligned} \tag{28}$$

(iv) when $|z| < 1$ and $|\varepsilon| \geq 1$,

$$\begin{aligned} \dot{V} &= -\alpha(z^2 + \varepsilon^{\frac{m}{n}+1}) - \beta(z^{\frac{p}{q}+1} + \varepsilon^{\frac{p}{q}+1}) \\ &\leq -\alpha((z^2)^{\frac{\frac{m}{n}+1}{2}} + (\varepsilon^2)^{\frac{\frac{m}{n}+1}{2}}) - \beta((z^2)^{\frac{\frac{p}{q}+1}{2}} + (\varepsilon^2)^{\frac{\frac{p}{q}+1}{2}}) \\ &\leq -\alpha_0 V^{\frac{\frac{m}{n}+1}{2}} - \beta_0 V^{\frac{\frac{p}{q}+1}{2}} \end{aligned} \tag{29}$$

where $\alpha_0 = 4\alpha$, $\beta_0 = 2^{\frac{\frac{p}{q}+1}{2}}\beta$. Thus, based on Lemma 1, one can easily prove that (19), (22) are stabilized within a fixed time. The upper bound of settling time is estimated by:

$$T_c < \frac{1}{\alpha_0}\frac{n}{\frac{m-n}{2}} + \frac{q}{\frac{q-p}{2}}\frac{1}{2\alpha}\ln(1 + \frac{2\alpha}{\beta_0}) \tag{30}$$

Therefore, the closed-loop system of (1), (9), (18), (21), and (24) is fixed-time stable and z converges to the origin within a fixed time independent of initial conditions. Then, the main control input η can be calculated according to (12). It demonstrates that the actual system states v_C and i_L will also track their desired values $v_{C,d}$ and $i_{L,d}$, respectively.

Remark 2: As can be seen in (30), the upper bound of convergence time only depends on the design parameters, indicating that the fixed-time stabilization can be guaranteed and that the convergence time can be preset in advance.

IV. Experimental Results

In this section, the proposed fast fixed-time disturbance observer-based backstepping control strategy is experimentally investigated for DC/DC boost converter feeding CPL in a DC modern grid. As illustrated in Fig. 2, experimental setup of a boost converter with resistive load and CPL comprised of a buck converter with resistive load is implemented using Semikron IGBT stack (SEMITEACH B6U+E1CIF+B6CI) and passive components. The dSPACE MicroLabBox with DS1202 PowerPC DualCore 2 GHz processor board is adopted to control the duty cycle of the switch and generate associated PWM for both boost and CPL converters such that the desired output voltage is tracked. The control diagram of the proposed method is illustrated in Fig. 3. Utilizing the measured signals

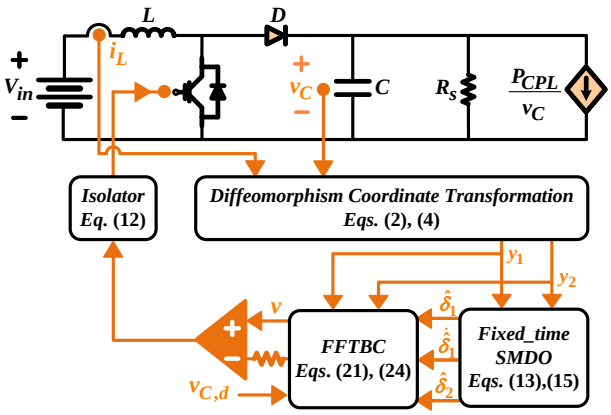

Fig. 3. The block diagram of the proposed fixed-time control scheme.

v_C and i_L, the diffeomorphism coordinate transformation in (2) and (4) including the total stored energy and rate of change of stored energy is applied. New state variables y_1 and y_2 are then received by the fixed-time SMDO in (13) and also by (15) in order to estimate the variation in load power and provide $\hat{\delta}_1$, $\dot{\hat{\delta}}_1$ and $\hat{\delta}_2$. The fast fixed-time backstepping controller including the virtual control expression y_2^* in (21) and the intermediate control law u in (24) is constructed by receiving the desired output voltage $v_{C,d}$, measurable signals y_1 and y_2 together with estimated values $\hat{\delta}_1$, $\dot{\hat{\delta}}_1$ and $\hat{\delta}_2$. Finally, the optimal value of the duty cycle of the switch, i.e., η in (12) is reached by employing isolator to the intermediate control law.

The electrical parameters for the boost converter are detailed in Table I. The observer and controller gains are tuned based on the mentioned theoretical analysis as $k_1 = k_2 = 0.5e3$, $k_3 = k_4 = 3.5e4$, $k_5 = k_6 = 50$, $\bar{m} = 0.8$, $\bar{n} = 1.2$, $\alpha_1 = \alpha_2 = 15$, $\beta_1 = \beta_2 = 295$, $p = 15$, $q = 33$, $m = 33$, $n = 15$.

It should be noticed that the larger observer design parameters $k_1 = k_2$ and $k_3 = k_4$ will result in a faster convergence rate for disturbance estimation. However, the overlarge values may give rise to some destructive effects, such as deriving overshoots. Regarding (13), it can be concluded that the variation of the third observer gain $k_5 = k_6$ does not influence the settling time. Moreover, when the tunable parameters of the proposed controller α_1, α_2, β_1 and β_2 become larger, the convergence speed for voltage regulation increases. The key issue is that the tunable parameters should be adopted such that a trade-off is made between the convergence rate and the smoothness of the control signal. Considering (30), the upper bound of settling time is estimated as $T_c < 1.6672$ *sec*, which is set in advance even if the initial condition is uncertain. To clarify the transient behavior of the results, data are imported into MATLAB workspace, and then the plots are depicted.

Study1: Performance validation under fast changes in CPL power, desired output voltage and input voltage

In practice, the CPLs are non-ideal with unknown and/or time-varying nature, which may cause system instability. Therefore, it is of major importance to guarantee the stable performance of the power electronic systems feeding non-ideal CPLs. This work provides a novel observer-based controller

TABLE I
SPECIFICATION OF THE BOOST CONVERTER

Parameters	Values
Inductance, L	$850\mu H$
Capacitance, C	$1100\mu F$
Switching frequency, f_s	$20kHz$
Converter input voltage, V_{in}	$48V$
DC bus voltage reference, $v_{C,d}$	$96V$

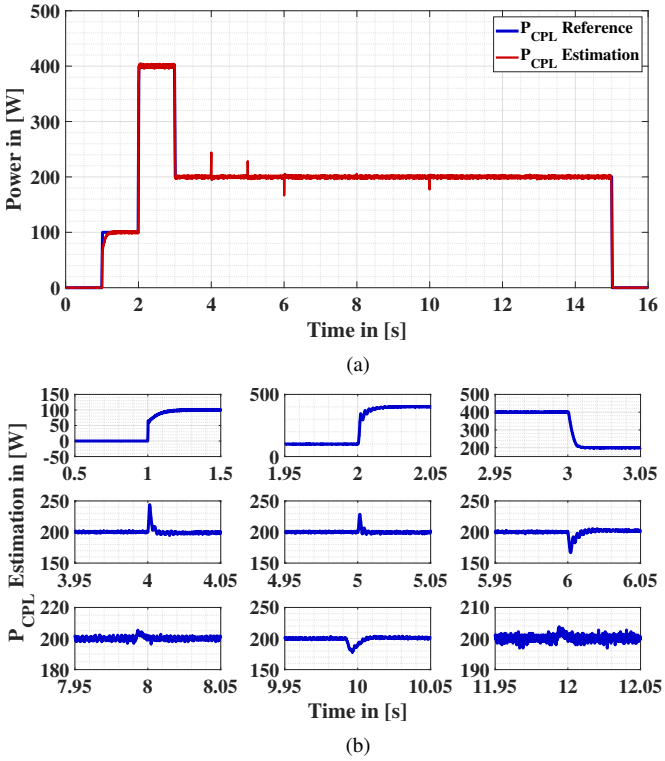

Fig. 4. Experimental results of the proposed FFTBC based on fixed-time SMDO: (a) CPL power, (b) transient responses of CPL power estimations.

against the power variations in the non-ideal CPLs as well as voltage variations in both input and desired output.

At first, it is assumed that CPL of $100W$, $400W$ and $200W$ is triggered in a fast-changing procedure at $1s$, $2s$ and $3s$, respectively. Then, when CPL power is $200W$, the desired output voltage decreases from $96V$ to $80V$ at $4s$, then decreases from $80V$ to $70V$ at $5s$ and finally increases from $70V$ to $96V$ at $6s$. Moreover, the input voltage is set as $62V$ for $t \in [8, 10)\ s$, $40V$ for $t \in [10, 12)\ s$, otherwise $48V$.

In Fig. 4(a), CPL power changes and its accurate estimation are displayed. Fig. 4(b) reveals the zoomed plot of the CPL power estimation at times when the sudden changes occur in CPL power, desired output voltage and input voltage. It is obvious that in the presence of fast changes ensued in CPL at $t = 1s$, $t = 2s$ and $t = 3s$, the estimated CPL power produced by the proposed fixed-time SMDO converge to its actual one within a fixed time about $100ms$, $20ms$ and $10ms$, respectively. It is noted that at times when the fast changes occur in both desired output voltage at $t = 4s$, $t = 5s$ and $t = 6s$ and input voltage at about $t = 8s$, $t = 10s$ and $t = 12s$, sudden errors occur in the estimated CPL power, which however are attenuated very fast in fixed time after $10ms$.

This article has been accepted for publication in IEEE Transactions on Industrial Electronics. This is the author's version which has not been fully edited and content may change prior to final publication. Citation information: DOI 10.1109/TIE.2022.3192669

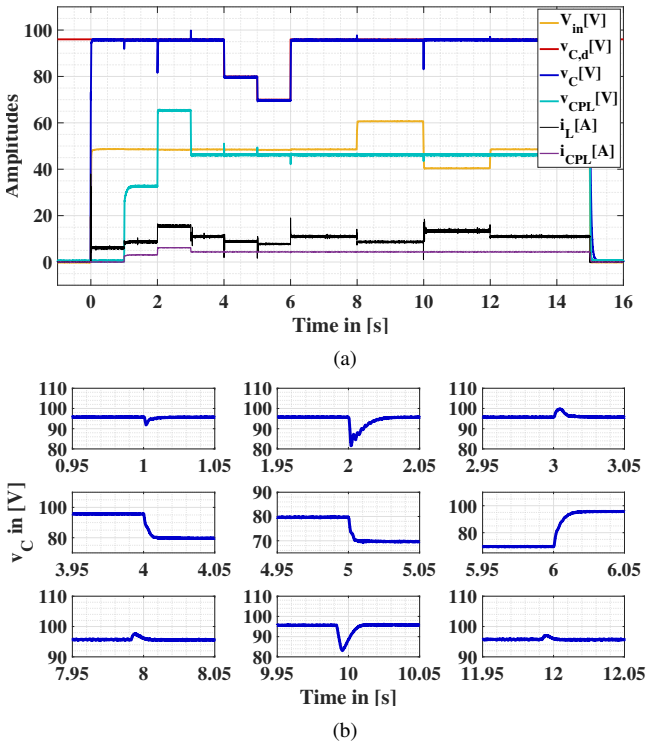

Fig. 5. Experimental results of the proposed FFTBC based on fixed-time SMDO: (a) voltage and current variations, (b) transient responses of v_C.

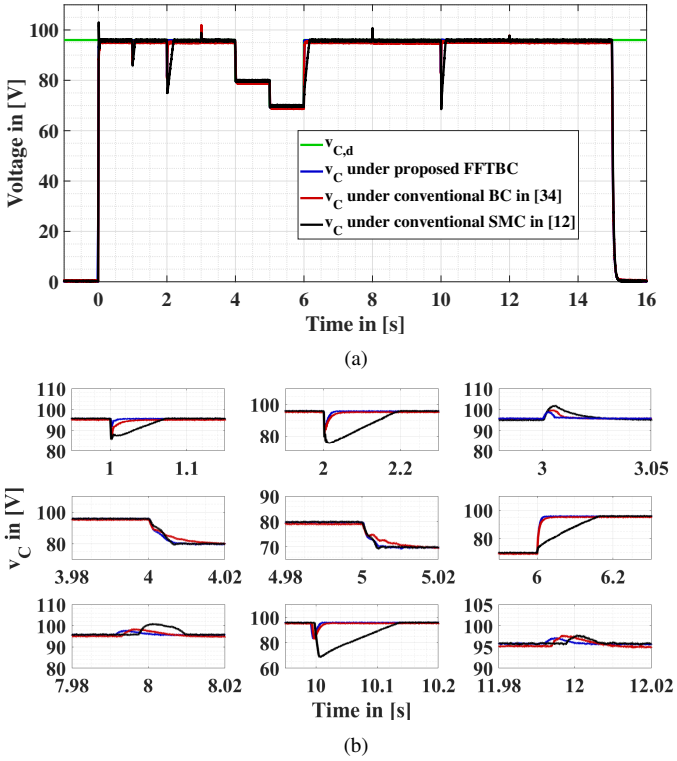

Fig. 6. Experimental results related to comparative study: (a) voltage variations, (b) transient responses of v_C under different controllers.

Fig. 5(a) presents the experimental results of the system with non-ideal CPL including dc bus voltage v_c, the CPL output voltage v_{CPL}, the inductor current i_L and CPL current i_{CPL}. One can observe from the zoomed plot in Fig. 5(b) that by utilizing the fast fixed-time backstepping controller based on fixed-time SMDO, the set-point of voltage term v_c remains at $96V$. However, it experiences deviations from its desired value at $t = 1s$, $t = 2s$ and $t = 3s$ which are eliminated abruptly after $10ms$, $30ms$, $10ms$, respectively. Moreover, the desired voltages are precisely tracked at $t = 4s$, $t = 5s$ and $t = 6s$ within a fixed-time less than $10ms$, $10ms$, $20ms$, respectively, which are independent of the initial conditions. The obtained results at the moments about $t = 8s$, $t = 10s$ and $t = 12s$ confirms the superiority of the proposed technique to restore desired values of the output voltage $v_{C,d}$ against time-varying input voltage V_{in} within a fixed time. In these moments, a small magnitude output voltage is observed, which are disappeared in less than $20ms$. Despite abrupt changes in CPL power, desired output voltage, and input voltage, one can see from Fig. 5(a) that the inductor current i_L follows its desired value within a fixed time by employing the proposed control scheme. It should be noted that the spike in the current waveform can be reduced by decreasing the controller parameters α and β. However, this may lead to slower convergence behavior for voltage regulation. Therefore, one should compromise between the convergence rate for regulating voltage and the smoothness of the current signals by accurately tuning the controller parameters. If the CPL current i_{CPL} is multiplied by the CPL output voltage v_{CPL}, the CPL power estimation depicted in Fig. 4(a) will be achieved.

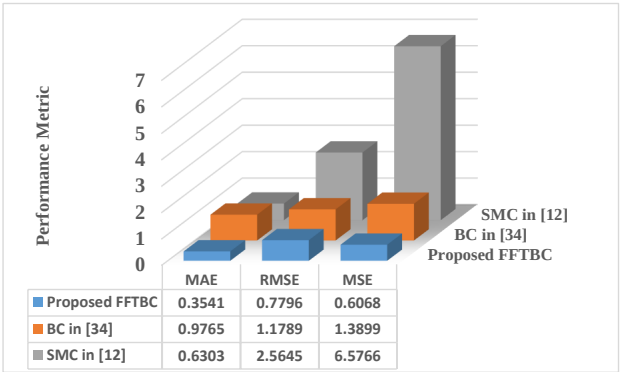

	MAE	RMSE	MSE
Proposed FFTBC	0.3541	0.7796	0.6068
BC in [34]	0.9765	1.1789	1.3899
SMC in [12]	0.6303	2.5645	6.5766

Fig. 7. Quantitative comparison of the controllers.

Study 2: Comparative study

A comparative research is conducted to assess the effectiveness of the proposed FFTBC based on fixed-time SMDO for restoring desired dc bus voltage. As revealed in Fig. 6(a), the conventional backstepping controller (BC) in [34] and also the conventional sliding-mode controller (SMC) in [12] is used to draw a comparison with the proposed fast fixed-time backstepping controller. Based on the zoomed plot in Fig. 6(b), the restoring process of desired voltage is faster with the lowest overshoots over the proposed FFTBC compared to two other controllers. In the presence of the instantaneous fast changes in the CPL power at $t = 1s$, $t = 2s$, $t = 3s$, the desired voltage set-point is restored within a fixed time, about $10ms$, using the proposed FFTBC. However, by employing the conventional BC in [34] and the conventional SMC in

[12], the convergence time increases to about $10ms$ and $0.2s$, respectively. The similar behavior can be found against desired output voltage variation at $t = 4s$, $t = 5s$, $t = 6s$ and abrupt changes in the input voltage at about $t = 8s$, $t = 10s$, $t = 12s$. The main reason is that these controllers in [34] and [12] only guarantee the asymptotical stability of the system. However, by applying the proposed fast fixed-time backstepping controller, the convergence time which is independent of the initial conditions can be preset offline. It can be seen from Fig. 6(b) that although the controllers in [34] and [12] can stabilize the output voltage v_C, its steady errors are more than $\%2$, while it is negligible under the proposed controller.

For a fair comparative study of the controllers in terms of quantity, some performance indexes including the mean square error (MSE), root mean square error (RMSE), and mean absolute error (MAE) are calculated to compare the performance of the proposed controller with two other control schemes [35]. The MSE represents the average of the squared difference between the actual values v_C and the desired ones $v_{C,d}$ in the data set, while the RMSE is the square root of the average of squared differences between them. Moreover, The MAE indicates the average of the absolute difference between the actual values v_C and the desired ones $v_{C,d}$ without considering their direction over all the data points. In Fig. 7, the bar plot corresponding to the performance analysis of the controllers is displayed. The MSE and RMSE indexes have the smallest values for the proposed FFTBC while they increase for BC in [34], and have the greatest values for SMC in [12]. Moreover, the value of the MAE is the smallest for the proposed FFTBC. There is an increase in the average of the absolute difference between the actual values v_C and the desired ones $v_{C,d}$ for SMC in [12], compared to the one for BC in [34]. Consequently, the lower values of MSE, RMSE, and MAE imply higher accuracy of the approach. Thus, the superiority of the proposed method is quantitatively confirmed.

V. Conclusion

This paper developed the fixed-time observer-based voltage regulating control for boost-based microgrid feeding unknown time-varying CPL. A fixed-time sliding mode disturbance observer was first designed to provide an estimation of the instantaneous power flow moving along the uncertain CPLs with time-varying nature within a fixed time. The sigmoid function exploited in the proposed observer structure enhances the estimation robustness against variation of the microgrid physical parameters. The fast fixed-time backstepping technique was then proposed based on the estimated load power to control the duty cycle of the boost converter such that the adverse effects of both nonlinear behavior and induced negative incremental impedance of the CPLs were mitigated. Thus, the desired voltage of the DC bus was tracked within a fixed time irrespective of the initial conditions. The upper bound of convergence time relies only on the design parameters which signifies the fixed-time stabilization can be guaranteed and the convergence time can be set in advance even if the initial condition is uncertain. To evaluate the practicability of the proposed technique over that of the other prevalent methods, a comparative study based on an experimental test-bed was implemented. The obtained results demonstrated the tracking ability of the proposed approach for DC microgrids despite abrupt variations in CPL power, desired output voltage, and input voltage. In order to enhance the performance of the system in the presence of large disturbances, the H_∞ norm can be considered in future research. Future research directions may focus on developing a fixed-time fault-tolerant control scheme for DC microgrids under faulty modes when failures in sensors, power switches, or controllers occur.

Appendix

Lemma 1: Consider the following differential equation:

$$\dot{y} = -ay^{\frac{1}{2}+\frac{r_1}{2r_2}+\left(\frac{r_1}{2r_2}-\frac{1}{2}\right)sign(|y|-1)} - by^{\frac{r_3}{r_4}} \tag{31}$$

where a and b are the positive real numbers and r_1, r_2, r_3, r_4 are positive odd integers that satisfy $r_1 > r_2$, $r_3 < r_4$. Then, the system (31) is fixed-time stable. The upper bound of settling time is estimated by $T_c < \frac{1}{a}\frac{r_2}{r_1-r_2} + \frac{r_4}{r_4-r_3}\frac{1}{a}\ln\left(1+\frac{a}{b}\right)$.

Proof: The system equation (31) can be simplified as:

$$\begin{cases} \dot{y} = -ay^{\frac{r_1}{r_2}} - by^{\frac{r_3}{r_4}}, & |y| > 1 \\ \dot{y} = -ay - by^{\frac{r_3}{r_4}}, & |y| < 1 \end{cases} \tag{32}$$

Assuming a new variable $w = y^{1-\frac{r_3}{r_4}}$, the first equation of system (32) can be developed as follows:

$$\dot{w} + \frac{r_4 - r_3}{r_4} a w^{\frac{\frac{r_1}{r_2}-\frac{r_3}{r_4}}{1-\frac{r_3}{r_4}}} + \frac{r_4 - r_3}{r_4} b = 0 \tag{33}$$

Define $\varsigma = [(r_1 - r_2)\, r_4]/[r_2\,(r_4 - r_3)]$, one can obtain:

$$\dot{w} + \frac{r_4 - r_3}{r_4} a w^{1+\varsigma} + \frac{r_4 - r_3}{r_4} b = 0 \tag{34}$$

The second equation of system (32) can be expressed as:

$$\dot{w} + \frac{r_4 - r_3}{r_4} a w + \frac{r_4 - r_3}{r_4} b = 0 \tag{35}$$

An upper-bound estimate for the settling time can be calculated by solving equations (34) and (35):

$$\begin{aligned} &\lim_{w_0\to\infty} T_c\,(w_0) = \lim_{w_0\to\infty} \tfrac{r_4}{r_4-r_3}\Big(\int_1^{w_0} \tfrac{1}{aw^{1+\varsigma}+b}dw + \int_0^1 \tfrac{1}{aw+b}dw\Big) \\ &< \lim_{w_0\to\infty} \tfrac{r_4}{r_4-r_3}\int_1^{w_0} \tfrac{1}{aw^{1+\varsigma}}dw + \tfrac{r_4}{a(r_4-r_3)}\ln(1+\tfrac{a}{b}) \\ &< \tfrac{r_4}{r_4-r_3}\big(\tfrac{1}{\varsigma a} + \tfrac{1}{a}\ln(1+\tfrac{a}{b})\big) = \tfrac{1}{a}\tfrac{r_2}{r_1-r_2} + \tfrac{r_4}{r_4-r_3}\tfrac{1}{a}\ln(1+\tfrac{a}{b}) \end{aligned} \tag{36}$$

Remark 3: For the suggested fixed-time stable system $\dot{y} = -ay^{\frac{r_1}{r_2}} - by^{\frac{r_3}{r_4}}$ where a and b are the positive real numbers and r_1, r_2, r_3, r_4 are positive odd integers that satisfy $r_1 > r_2$, $r_3 < r_4$, it is proved that the upper bound of settling time is calculated by $T_{c1} < \frac{1}{a}\frac{r_2}{r_1-r_2} + \frac{1}{b}\frac{r_4}{r_4-r_3}$ [36]. The fixed-time stable system in Lemma 1 expedites the convergence rate such that the upper bound of settling time is estimated by $T_{c2} < \frac{1}{a}\frac{r_2}{r_1-r_2} + \frac{r_4}{r_4-r_3}\frac{1}{a}\ln\left(1+\frac{a}{b}\right)$. Since the inequality $Ln\left(1+\frac{a}{b}\right) \le \frac{a}{b}$ holds, one can get $T_{c2} < T_{c1}$. If the state of the system is close to the equilibrium point, i.e. $|y| < 1$ in (32), using a linear term y instead of the nonlinear term $y^{\frac{r_1}{r_2}}$ causes to faster convergence rate.

Lemma 2 [37]: For any non-negative real numbers ξ_1, ξ_2, ..., ξ_n the inequality $\sum_{i=1}^{n} \xi_i^p \geq (\sum_{i=1}^{n} \xi_i)^p$ holds for any $0 < p \leq 1$ while $\sum_{i=1}^{n} \xi_i^p \geq n^{1-p}(\sum_{i=1}^{n} \xi_i)^p$ holds for any $p > 1$.

REFERENCES

[1] W. Li, A. Monti, and F. Ponci, "Fault detection and classification in medium voltage dc shipboard power systems with wavelets and artificial neural networks," *IEEE Transactions on Instrumentation and Measurement*, vol. 63, no. 11, pp. 2651–2665, 2014.

[2] G. Buticchi, S. Bozhko, M. Liserre, P. Wheeler, and K. Al-Haddad, "On-board microgrids for the more electric aircraft," *IEEE Transactions on Industrial Electronics*, vol. 66, no. 7, pp. 5588–5599, 2018.

[3] M. H. Khooban, N. Vafamand, T. Niknam, T. Dragicevic, and F. Blaabjerg, "Model-predictive control based on takagi-sugeno fuzzy model for electrical vehicles delayed model," *IET Electric Power Applications*, vol. 11, no. 5, pp. 918–934, 2017.

[4] N. Sarrafan, M. A. Rostami, J. Zarei, R. Razavi-Far, M. Saif, and T. Dragicevic, "Improved distributed prescribed finite-time secondary control of inverter-based microgrids: Design and real-time implementation," *IEEE Transactions on Industrial Electronics*, 2020.

[5] A. Bidram and A. Davoudi, "Hierarchical structure of microgrids control system," *IEEE Transactions on Smart Grid*, vol. 3, no. 4, pp. 1963–1976, 2012.

[6] J. Kumar, A. Agarwal, and V. Agarwal, "A review on overall control of DC microgrids," *Journal of energy storage*, vol. 21, pp. 113–138, 2019.

[7] O. D. Montoya, "On linear analysis of the power flow equations for DC and AC grids with CPLs," *IEEE Transactions on Circuits and Systems II: Express Briefs*, vol. 66, no. 12, pp. 2032–2036, 2019.

[8] M. Cespedes, L. Xing, and J. Sun, "Constant-power load system stabilization by passive damping," *IEEE Transactions on Power Electronics*, vol. 26, no. 7, pp. 1832–1836, 2011.

[9] X. Zhang, X. Ruan, and Q.-C. Zhong, "Improving the stability of cascaded DC/DC converter systems via shaping the input impedance of the load converter with a parallel or series virtual impedance," *IEEE Transactions on Industrial Electronics*, vol. 62, no. 12, pp. 7499–7512, 2015.

[10] J. A. Solsona, S. G. Jorge, and C. A. Busada, "Nonlinear control of a buck converter which feeds a constant power load," *IEEE Transactions on Power Electronics*, vol. 30, no. 12, pp. 7193–7201, 2015.

[11] S. Arora, P. Balsara, and D. Bhatia, "Input–output linearization of a boost converter with mixed load (constant voltage load and constant power load)," *IEEE Transactions on Power Electronics*, vol. 34, no. 1, pp. 815–825, 2018.

[12] Y. Zhao, W. Qiao, and D. Ha, "A sliding-mode duty-ratio controller for DC/DC buck converters with constant power loads," *IEEE Transactions on industry Applications*, vol. 50, no. 2, pp. 1448–1458, 2013.

[13] S. Singh, D. Fulwani, and V. Kumar, "Robust sliding-mode control of DC/DC boost converter feeding a constant power load," *IET Power Electronics*, vol. 8, no. 7, pp. 1230–1237, 2015.

[14] M. Alipour, J. Zarei, R. Razavi-Far, M. Saif, N. Mijatovic, and T. Dragicevic, "Observer-based backstepping sliding mode control design for microgrids feeding a constant power load," *IEEE Transactions on Industrial Electronics*, DOI: 10.1109/TIE.2022.3152028, 2022.

[15] Q. Xu, C. Zhang, C. Wen, and P. Wang, "A novel composite nonlinear controller for stabilization of constant power load in DC microgrid," *IEEE Transactions on Smart Grid*, vol. 10, no. 1, pp. 752–761, 2017.

[16] X. Li, X. Zhang, W. Jiang, J. Wang, P. Wang, and X. Wu, "A novel assorted nonlinear stabilizer for DC-DC multilevel boost converter with constant power load in DC microgrid," *IEEE Transactions on Power Electronics*, vol. 35, no. 10, pp. 11 181–11 192, 2020.

[17] E. Kowsari, J. Zarei, R. Razavi-Far, M. Saif, T. Dragičević, and M. H. Khooban, "A novel stochastic predictive stabilizer for DC microgrids feeding CPLs," *IEEE Journal of Emerging and Selected Topics in Power Electronics*, 2020.

[18] N. Vafamand, M. H. Khooban, T. Dragičević, F. Blaabjerg, and J. Boudjadar, "Robust non-fragile fuzzy control of uncertain DC microgrids feeding constant power loads," *IEEE Transactions on Power Electronics*, vol. 34, no. 11, pp. 11 300–11 308, 2019.

[19] N. Vafamand, M. H. Khooban, T. Dragičević, and F. Blaabjerg, "Networked fuzzy predictive control of power buffers for dynamic stabilization of DC microgrids," *IEEE Transactions on Industrial Electronics*, vol. 66, no. 2, pp. 1356–1362, 2018.

[20] C. Cui, N. Yan, B. Huangfu, T. Yang, and C. Zhang, "Voltage regulation of DC-DC buck converters feeding CPLs via deep reinforcement learning," *IEEE Transactions on Circuits and Systems II: Express Briefs*, vol. 69, no. 3, pp. 1777–1781, 2021.

[21] M. A. Hassan, E.-P. Li, X. Li, T. Li, C. Duan, and S. Chi, "Adaptive passivity-based control of DC-DC buck power converter with constant power load in DC microgrid systems," *IEEE Journal of Emerging and Selected Topics in Power Electronics*, vol. 7, no. 3, pp. 2029–2040, 2018.

[22] Q. Xu, F. Blaabjerg, and C. Zhang, "Finite-time stabilization of constant power loads in DC microgrids," in *2019 IEEE Energy Conversion Congress and Exposition (ECCE)*. IEEE, 2019, pp. 2059–2064.

[23] Q. Xu, C. Zhang, Z. Xu, P. Lin, and P. Wang, "A composite finite-time controller for decentralized power sharing and stabilization of hybrid fuel cell/supercapacitor system with constant power load," *IEEE Transactions on Industrial Electronics*, vol. 68, no. 2, pp. 1388–1400, 2020.

[24] M. Asghar, A. Khattak, M. M. Rafiq *et al.*, "Comparison of integer and fractional order robust controllers for DC/DC converter feeding constant power load in a DC microgrid," *Sustainable Energy, Grids and Networks*, vol. 12, pp. 1–9, 2017.

[25] N. Sarrafan, J. Zarei, R. Razavi-Far, M. Saif, and M.-H. Khooban, "A novel on-board DC/DC converter controller feeding uncertain constant power loads," *IEEE Journal of Emerging and Selected Topics in Power Electronics*, 2020.

[26] S. Sumsurooah, M. Odavic, and S. Bozhko, "μ approach to robust stability domains in the space of parametric uncertainties for a power system with ideal CPL," *IEEE Transactions on Power Electronics*, vol. 33, no. 1, pp. 833–844, 2017.

[27] J. Liu, W. Zhang, and G. Rizzoni, "Robust stability analysis of DC microgrids with constant power loads," *IEEE Transactions on Power Systems*, vol. 33, no. 1, pp. 851–860, 2017.

[28] H. Amiri, G. A. Markadeh, and N. M. Dehkordi, "Voltage control in a DC islanded microgrid based on nonlinear disturbance observer with CPLs," *Journal of Energy Storage*, vol. 29, p. 101296, 2020.

[29] M. K. AL-Nussairi, R. Bayindir, S. Padmanaban, L. Mihet-Popa, and P. Siano, "Constant power loads (CPL) with microgrids: Problem definition, stability analysis and compensation techniques," *Energies*, vol. 10, no. 10, p. 1656, 2017.

[30] H. Sira-Ramirez and M. Ilic-Spong, "Exact linearization in switched-mode DC-to-DC power converters," *International journal of control*, vol. 50, no. 2, pp. 511–524, 1989.

[31] J. Ni, L. Liu, M. Chen, and C. Liu, "Fixed-time disturbance observer design for brunovsky systems," *IEEE Transactions on Circuits and Systems II: Express Briefs*, vol. 65, no. 3, pp. 341–345, 2017.

[32] J. Sun, J. Yi, Z. Pu, and X. Tan, "Fixed-time sliding mode disturbance observer-based nonsmooth backstepping control for hypersonic vehicles," *IEEE Transactions on Systems, Man, and Cybernetics: Systems*, vol. 50, no. 11, pp. 4377–4386, 2018.

[33] Y. Zhang, C. Hua, and K. Li, "Disturbance observer-based fixed-time prescribed performance tracking control for robotic manipulator," *International Journal of Systems Science*, vol. 50, no. 13, pp. 2437–2448, 2019.

[34] S. Yousefizadeh, J. D. Bendtsen, N. Vafamand, M. H. Khooban, F. Blaabjerg, and T. Dragičević, "Tracking control for a DC microgrid feeding uncertain loads in more electric aircraft: Adaptive backstepping approach," *IEEE Transactions on Industrial Electronics*, vol. 66, no. 7, pp. 5644–5652, 2018.

[35] J. Zarei and E. Shokri, "Convergence analysis of non-linear filtering based on cubature kalman filter," *IET Science, Measurement & Technology*, vol. 9, no. 3, pp. 294–305, 2015.

[36] Z. Zuo, "Non-singular fixed-time terminal sliding mode control of non-linear systems," *IET control theory & applications*, vol. 9, no. 4, pp. 545–552, 2015.

[37] Z. Zuo and L. Tie, "A new class of finite-time nonlinear consensus protocols for multi-agent systems," *International Journal of Control*, vol. 87, no. 2, pp. 363–370, 2014.

Neda Sarrafan received her B.Sc. degree in telecommunication engineering and M.Sc. degree in control engineering in 2012 and 2015, respectively. Since 2017, she has been a Ph.D. student in control engineering in Shiraz University of Technology, Shiraz, Iran. Her main research interests include nonlinear control theory and applications, cooperative control of multi-agent systems, collaborative robotics, fault tolerant control systems, cyber-physical systems, stability analysis and control of power systems.

Jafar Zarei ($S'10, M'14$) received the B.S. degree in electrical engineering from Shiraz University, Shiraz, Iran, in 2002, and the M.Sc. and Ph.D. degrees in electrical engineering from the Iran University of Science and Technology, Tehran, Iran, in 2005, and 2011, respectively. Since 2011, he has been with Shiraz University of Technology, Shiraz, where he is currently an Associate Professor with the Department of Electrical and Electronics Engineering. He has been a Research Associate with the Faculty of Engineering, University of Windsor, Windsor, ON, Canada, since August 2019.

His research interests include on the theoretical side, estimation theory, robust control, analysis, and control of networked control systems (fuzzy, Markovian jump models), cyber-physical systems, fault detection and isolation, fault-tolerant control, analysis, and control via linear matrix inequality optimization techniques, and Lyapunov-based methods. On the application side, he is mainly interested in control design for microgrids, and condition monitoring and fault detection of induction motors. He is currently an Associate Editor of the Iranian Journal of Science and Technology: Transaction of Electrical Engineering.

Navid Horiyat received his B.Sc. degree in 2011 and M.Sc.s degree in 2014, both in Electrical Engineering. Since 2017, he has been with the control research group in the Shiraz University of Technology, Shiraz, Iran. His main research interests include the design of electrical machines, chaos theory in electrical power systems, fault diagnosis of electrical machines, power system stabilizers, power electronics and control of power systems.

Roozbeh Razavi-Far ($S'08 - M'17 - SM'19$) received the B.Sc. degree in Electrical and Computer Engineering, the M.Sc. and Ph.D. degrees from the Amirkabir University of Technology and achieved a second Ph.D. degree from Politecnico di Milano. He was a postdoctoral fellow at the Université Libre de Bruxelles, Belgium, an NSERC postdoctoral fellow at NRCan Federal Laboratories, and a lecturer and postdoctoral fellow at the University of Windsor, Canada. He is currently with the Faculty of Engineering at the University of Windsor.

Mehrdad Saif ($S'84 - M'84 - SM'05$) received the B.S., M.S., and D.Eng. degrees in electrical engineering from Cleveland State University, Cleveland, OH, USA, in 1982, 1984, and 1987, respectively. He has been the Dean of the Faculty of Engineering, University of Windsor, Windsor, ON, Canada, since July 2011. His research interests include systems and control; estimation and observer theory; model based fault diagnostics; condition monitoring, diagnostics and prognostic; and application of these areas to automotive, power, and autonomous systems.

Nenad Mijatovic After obtaining his Dipl.Ing. education in Electrical Power Engineering at University of Belgrade, Serbia in 2007, was enrolled as a doctoral candidate at Technical University of Denmark. He received his Ph.D. degree from Technical University of Denmark. Upon completion of his PhD, he continued work within the field of wind turbine direct-drive concepts as an Industrial PostDoc. Dr. N. Mijatovic currently holds position of Associate Professor at Technical University of Denmark.

Tomislav Dragičević ($S'09 - M'13 - SM'17$) received the M.Sc. and the industrial Ph.D. degrees in Electrical Engineering from the Faculty of Electrical Engineering, University of Zagreb, Croatia, in 2009 and 2013, respectively. From 2013 until 2016 he has been a Postdoctoral researcher at Aalborg University, Denmark. From 2016 until 2020 he was an Associate Professor at Aalborg University, Denmark. From 2020 he is a Professor at the Technical University of Denmark.